



# Rapid selection of analytical lines for SAF-LIBS based on the doublet intensity ratios at the initial and final stages of plasma

J. J. HOU,<sup>1,2</sup> L. ZHANG,<sup>1,2,\*</sup> Y. ZHAO,<sup>1,2</sup> W. G. MA,<sup>1,2</sup>  L. DONG,<sup>1,2</sup> W. B. YIN,<sup>1,2,\*</sup> L. T. XIAO,<sup>1,2</sup> AND S. T. JIA<sup>1,2</sup>

<sup>1</sup>State Key Laboratory of Quantum Optics and Quantum Optics Devices, Institute of Laser Spectroscopy, Shanxi University, Taiyuan 030006, China

<sup>2</sup>Collaborative Innovation Center of Extreme Optics, Shanxi University, Taiyuan 030006, China

\*k1226@sxu.edu.cn

**Abstract:** Self-absorption-free laser-induced breakdown spectroscopy (SAF-LIBS) can directly obtain the applicable quasi-optically thin lines by determining the optimal acquisition delay time according to the intensity ratio of doublet lines at specific transition wavelength of the analyzed elements, thus eliminating the influence of self-absorption on quantitative results. In quantitative analysis of samples with a certain content range, the key to the convenient application of this technique is to rapidly select the suitable doublet lines for the element to be analyzed. The theoretical analysis shows that the evolution trend of doublet intensity ratio is monotonous under the assumptions that the plasma is uniform and in local thermal equilibrium (LTE) and the area density ( $Nl$ ) is a constant, which is also confirmed by the experimental results of Cu and Al. Thus, a rapid spectral line selection criterion for SAF-LIBS applications is derived: only when the doublet intensity ratios measured at the initial and final stages of plasma induced by the boundary sample with the highest element content lie on both sides of the theoretical ratio, the doublet lines can reach quasi-optically thin during plasma evolution and are suitable for SAF-LIBS measurements. This new criterion is helpful to promote the practicality and industrial application of SAF-LIBS technology.

© 2019 Optical Society of America under the terms of the [OSA Open Access Publishing Agreement](#)

## 1. Introduction

Laser-induced breakdown spectroscopy (LIBS) is a technique for qualitative and quantitative analysis of material composition by analyzing the spectral information of laser-induced plasma [1–7]. Fundamentally, a plasma is optically thin when the emitted radiation traverses and escapes from the plasma without significant absorption or scattering [8]. In the case of high density plasma, there exists a self-absorption effect that the outward emission is reabsorbed by the plasma itself, which decreases the intensity of radiation and broadens the spectral line width [9,10]. Therefore, eliminating self-absorption to obtain quasi-optically thin spectral lines is essential for accurate LIBS measurement. In order to correct or even eliminate self-absorption, a lot of research work has been carried out in the past decades. Sherbini *et al.* [11] proposed a method to correct self-absorption effect by using the line width to calculate the self-absorption (SA) coefficient of emission line, and verified that the systematic error of electron temperature caused by the uncorrected line intensity could be avoided. Sun *et al.* [12] utilized an internal reference line to correct self-absorption effect in calibration-free LIBS (CF-LIBS), and found that both linearity of Boltzmann plot and accuracy of quantitative analysis were improved. Alfarraj *et al.* [13] used the curve of growth to determine the optical depth and self-absorption of Sr and Al lines by evaluating the plasma temperature and the parameter  $Nl$  (number density  $N$  and absorption path length  $l$ ). Wang *et al.* [14] proposed a blackbody radiation referenced method to correct self-absorption in CF-LIBS through the theoretical blackbody radiation, and both

linearity of Boltzmann plot and measurement accuracy were improved. We recently proposed a self-absorption-free LIBS (SAF-LIBS) technique [15], which optimizes the delay time of spectra acquisition by using the intensity ratio of doublet lines, to directly capture the quasi-optically thin emission lines. Univariate quantitative analysis showed that the average absolute measurement error was reduced by nearly one order of magnitude compared with the conventional LIBS. Furthermore, combined with resonance and nonresonance doublets [16], SAF-LIBS was proved to be able to provide accurate chemical composition measurements within a wide range of element content. However, in the above studies, we found that for SAF-LIBS, different doublets have different maximum detectable element contents. For example, the maximum detectable Al content is 15.9% by using the Al I 396.15 nm and 394.40 nm doublet, while it is 13.1% by using the Al I 309.27 nm and 308.21 nm doublet. Therefore, in quantitative analysis of samples with a certain content range, the key to the convenient application of this technique is to rapidly select the suitable doublet lines for the element to be analyzed.

In order to better understand the principle of doublet intensity ratio and obtain a simple and rapid spectral line selection criterion for SAF-LIBS, this paper theoretically analyzes the self-absorption process in plasma and the trends of doublet intensity ratio at different transitions.

## 2. Theoretical

### 2.1. Self-absorption

The self-absorption coefficient  $SA$  is defined as the ratio of the actual intensity  $I(\lambda_0)$  of the emission line at its maximum over the value  $I_0(\lambda_0)$  obtained by extrapolating the curve of growth valid in the optically thin regime to the same emitters number density of the actual measurement [11,17]:

$$SA = \frac{I(\lambda_0)}{I_0(\lambda_0)} = \frac{(1 - e^{-k(\lambda_0)l})}{k(\lambda_0)l} = \frac{(1 - e^{-K/\Delta\lambda_0})}{K/\Delta\lambda_0}, \quad (1)$$

where  $k(\lambda_0)$  is the absorption coefficient, and  $l$  is the length of the absorption path. The  $k(\lambda_0)l$ , also called as optical depth, determines the self-absorption degree of the line. The  $\Delta\lambda_0$  is the expected full width at half maximum (FWHM) of the emission line and since the Lorentzian width of line is mainly dominated by the Stark broadening effect, the FWHMs are the same for lines with the same upper energy level belonging to the same multiplet [10].  $K = 2 \frac{e^2}{mc^2} n_i f \lambda_0^2 l$ , where  $e$  is the electron charge,  $m$  is the electron mass,  $c$  is the light speed,  $n_i$  is the number density of species in the  $i$  level, and  $f$  is the transition oscillator strength. From Eq. (1), it can be inferred that  $SA$  decreases with the increase of  $K$ , which means that if  $\Delta\lambda_0$  does not change with time, the larger the  $K$ , the more self-absorbed the emission line. Combined with the Boltzmann distribution law and the relationship between oscillator strength and transition probability (the Ladenburg formula),  $K$  can be expressed as [18]:

$$\begin{aligned} K &= \frac{Nl}{4\pi^2 c} \frac{Agk\lambda_0^4}{Z(T)} e^{-\frac{E_i}{k_B T}} \\ &= C_0 Agk\lambda_0^4 \frac{e^{-\frac{E_i}{k_B T}}}{g_1 e^{-\frac{E_1}{k_B T}} + g_2 e^{-\frac{E_2}{k_B T}} + \dots + g_j e^{-\frac{E_j}{k_B T}} + \dots}, \end{aligned} \quad (2)$$

where  $N$  is the total number density of species in an atomic or ionic state,  $A$  is the transition probability,  $Z(T)$  is the partition function,  $E_i$  is the lower level energy,  $k_B$  is the Boltzmann constant, and  $T$  is the plasma temperature. For simplicity, assuming the area density  $Nl$  is a constant and does not change with time, and then  $C_0$  is a constant for the same species. It can be seen from the above equations that self-absorption is positively correlated with transition probability, degeneracy of upper level, wavelength, number density and length of the absorption

path, and is negatively correlated with lower energy level. Note that the relationship between self-absorption and temperature varies with energy level.  $SA$  decreases with the decrease of plasma temperature if the lower level is in the ground state, while increases with the decrease of plasma temperature if the lower level is in a relatively high excited state.

It should also be noted that the effect of self-absorption on the measured line integral intensity  $\bar{I}(\lambda)$  can also be numerically evaluated in terms of  $SA$  and the non-self-absorbed integral intensity  $\bar{I}_0(\lambda)$  as:

$$\frac{\bar{I}(\lambda)}{\bar{I}_0(\lambda)} = (SA)^\beta, \quad (3)$$

with  $\beta=0.46$ .

## 2.2. Doublet intensity ratio

Assuming the plasma is uniform, optically thin and in local thermodynamic equilibrium (LTE) during spectra acquisition, the theoretical doublet integrated intensity ratio of an element in the ionization stage  $Z$  can be expressed as:

$$\frac{\bar{I}_{1,0}}{\bar{I}_{2,0}} = \left(\frac{\lambda_{nm,Z}}{\lambda_{ki,Z}}\right) \left(\frac{A_{ki,Z}}{A_{nm,Z}}\right) \left(\frac{g_{k,Z}}{g_{n,Z}}\right) \exp\left(-\frac{E_{k,Z} - E_{n,Z}}{k_B T}\right), \quad (4)$$

where  $\bar{I}_{1,0}$  is the line integral intensity from the  $k$ - $i$  transition and  $\bar{I}_{2,0}$  is that from the  $n$ - $m$  transition, and define  $\bar{I}_{1,0}$  to be greater than  $\bar{I}_{2,0}$ . When the doublet lines have the same or comparable upper levels, the temperature dependent exponential item can be ignored and this intensity ratio tends to be a constant independent of time and experimental conditions. By matching this ratio with the measured values at different delay times, the exact time window where the spectral line is closest to be quasi-optically thin can be found, thus realizing SAF-LIBS.

From Eqs. (3) and (4), we easily obtain:

$$\frac{\bar{I}_1}{\bar{I}_2} = \frac{\bar{I}_{1,0} SA_1^\beta}{\bar{I}_{2,0} SA_2^\beta} = C_1 \left(\frac{SA_1}{SA_2}\right)^\beta, \quad (5)$$

where  $C_1$  is a constant dependent on Eq. (4).

In the case of very weak self-absorption,  $k_{1,2}(\lambda_0)l \ll 1$  and  $SA$  approximates to 1, so that the doublet intensity ratio of the same species becomes  $\frac{\bar{I}_1}{\bar{I}_2} \approx C_1$ . Therefore, when the measured doublet intensity ratio is equal to the theoretical value at a certain delay, the spectral line at  $\lambda_0$  can be regarded as optically thin.

## 2.3. Trend of doublet intensity ratio

The trend of doublet intensity ratio is related to the selected spectral lines and acquisition conditions. Provided that  $K$  is a function of time  $t$ , i.e.  $K=f(t)$ . According to Eq. (5), the trend of doublet intensity ratio can be predicted by its first order derivative with respect to time as:

$$\left(\frac{\bar{I}_1}{\bar{I}_2}\right)' = C_1 \frac{d(SA_1^\beta / SA_2^\beta)}{dt} = C_1 \beta \left(\frac{SA_1}{SA_2}\right)^{\beta-1} \left(\frac{(SA_1)'SA_2 - SA_1(SA_2)'}{SA_2^2}\right). \quad (6)$$

It can be seen that the trend depends on whether the value of  $(SA_1)'SA_2 - SA_1(SA_2)'$  is greater or less than zero. Specifically, for the doublet intensity ratio, the two spectral lines have the same state and transition energy level, which would give  $K_2 = C_2 K_1$ . Here provided  $\bar{I}_1$  is greater than  $\bar{I}_2$ , then  $C_2 < 1$ . So, putting  $x = K_1 / \Delta\lambda_0$ , which reflects the degree of self-absorption, we obtain

the following derivative formulas:

$$(SA_1)' = \frac{(K_1 + \Delta\lambda_0)e^{-K_1/\Delta\lambda_0} - \Delta\lambda_0}{K_1^2} \times K_1' = \frac{(x+1)e^{-x} - 1}{\Delta\lambda_0 x^2} \times K_1', \quad (7)$$

$$(SA_2)' = \frac{(K_2 + \Delta\lambda_0)e^{-K_2/\Delta\lambda_0} - \Delta\lambda_0}{K_2^2} \times K_2' = \frac{(C_2x+1)e^{-C_2x} - 1}{\Delta\lambda_0 C_2 x^2} \times K_1', \quad (8)$$

$$(SA_1)'SA_2 - SA_1(SA_2)' = \frac{[e^{-x}(1 - e^{-C_2x}) - C_2e^{-C_2x}(1 - e^{-x})]}{C_2K_1^2} \times \Delta\lambda_0 K_1'. \quad (9)$$

In LIBS experiments, the plasma temperature  $T$  usually decreases with time. And the relationship of  $K$  with respect to  $T$  can be easily obtained through a simple data-curve fitting approach. If  $K$  decreases with the decrease of  $T$ , that is,  $K$  decreases with time, then  $K' < 0$ . On the contrary, if  $K$  increase with the decrease of  $T$ , then  $K' > 0$ .

### 3. Experimental

Here, the whole experimental LIBS setup is briefly summarized, which has been described in detail in the previous work [15,16]. The ablation source was a 1064 nm Q-switched Nd: YAG laser (Spectral Physics, INDI-HG-20S), with a pulse duration of 7 ns, a repetition rate of 20 Hz and a fixed energy of 50 mJ/pulse. The laser beam was focused at the sample surface by an objective lens with a focal length of 75 mm, and the diameter of the focal spot was approximately 600  $\mu\text{m}$ . A condenser lens with a focal length of 75 mm was aligned with the laser-produced plasma to generate a 4 $\times$  magnified plume image. Then the image along the line of sight perpendicular to the laser beam was delivered to a grating spectrograph (Princeton Instruments, SP-2750) that equipped with a time gated ICCD (Princeton Instruments, PI-MAX4-1024i) by use of a 200  $\mu\text{m}$  optical fiber.

In our experiment, the quasi-optically thin spectra of doublet Cu I 521.82 and 515.32 nm lines (non-resonance transition:  $3d^{10}4d-3d^{10}4p$ ) and doublet Al I 396.15 and 394.40 nm lines (resonance transition:  $3s^24s-3s^23p$ ) were captured by SAF-LIBS, and the evolution trends of doublet intensity ratio were investigated. The samples used in the experiment included six homemade pressed tablets of pure finely powdered potassium bromide and copper oxide with Cu content of  $3 \pm 0.27$ ,  $9 \pm 0.09$ ,  $12 \pm 0.17$ ,  $15 \pm 0.05$ ,  $30 \pm 0.03$ , and  $60 \pm 0.01\%$  (wt/wt), and nine homemade pressed tablets of pure finely powdered potassium bromide and aluminum oxide with Al content of  $5 \pm 0.11$ ,  $6 \pm 0.09$ ,  $7 \pm 0.08$ ,  $8 \pm 0.07$ ,  $9 \pm 0.06$ ,  $10 \pm 0.05$ ,  $11 \pm 0.05$ ,  $13 \pm 0.04$ , and  $19 \pm 0.03\%$  (wt/wt). The detailed spectroscopic parameters are listed in Table 1, taken from the NIST atomic database. The measured  $T$  ranged from 8000 K to 12000K in this experiment and decreased with time. All the spectra were obtained by averaging 60 measurements with background subtracted under identical experimental conditions.

**Table 1. Spectroscopic parameters of the Cu I and Al I doublets.**

Species	Wavelength (nm)	Transition Probability ( $\text{sec}^{-1}$ )	Statistical Weight	Upper Level Energy (eV)	Lower Level Energy (eV)
Cu I	515.32	$6.00 \times 10^7$	4	6.19	3.79
	521.82	$7.50 \times 10^7$	6	6.19	3.82
Al I	394.40	$4.99 \times 10^7$	2	3.14	0.00
	396.15	$9.85 \times 10^7$	2	3.14	0.01

## 4. Results and discussion

### 4.1. Evolution of doublet Cu I intensity ratio

According to Eq. (2), the numerical fitting curve of  $K$  versus  $T$  corresponding to Cu I 521.82 nm is shown as red solid curve in Fig. 1, with a step of 1000 K in the range of 5000 K to 15000 K. It can be seen that  $K$  decreases with the decrease of  $T$ , that is,  $K$  decreases with time, so  $K' < 0$ . Then the derivative of the ratio  $I_{\text{Cu } 521.82 \text{ nm}}/I_{\text{Cu } 515.32 \text{ nm}}$  with respect to time was determined by Eq. (9), where  $C_2=0.54$ . Denote  $(SA_1)'SA_2 - SA_1(SA_2)'$  as  $y$ , Fig. 2 shows the relationship of  $y$  with respect to  $x$  as red solid curve for the Cu I doublet. It can be seen that  $y$  is always positive, and tends to be zero when  $x$  is low to 0 (optically thin) or higher than 20 (serious self-absorption), which means that, in theory, the doublet ratio of Cu I increases with time and the trend tends to be zero in the case of optically thin or serious self-absorption. Therefore, the doublet Cu I intensity ratio rises with time, and its trend tends to zero as the self-absorption decreases to optically thin. Then it begins to rise again with the increase of self-absorption until the change tends to zero when the self-absorption is serious.

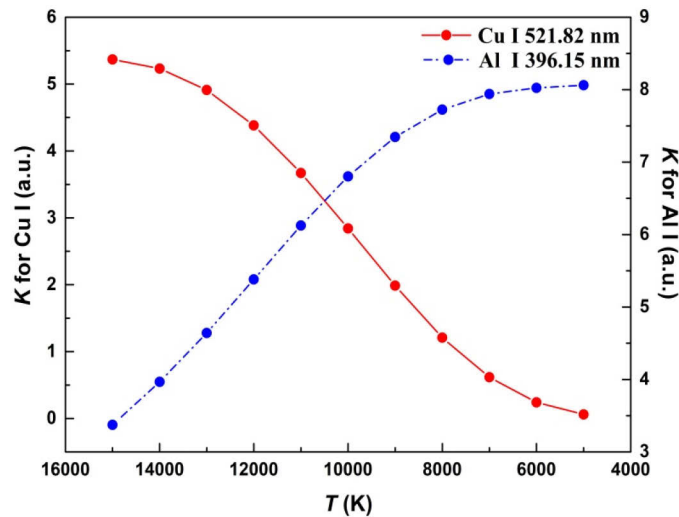
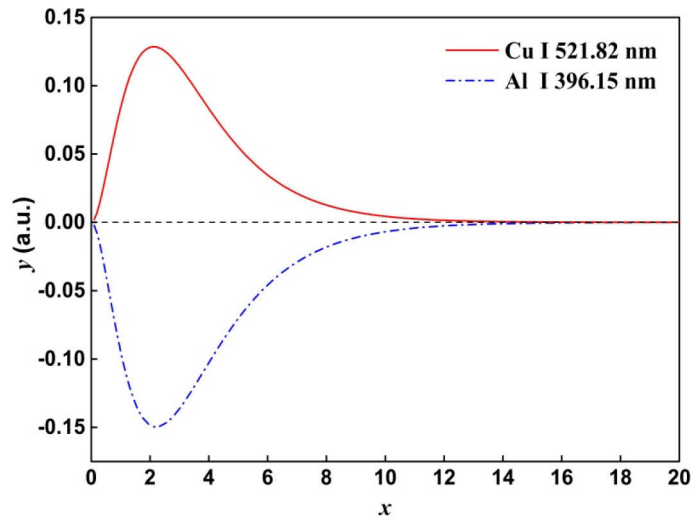


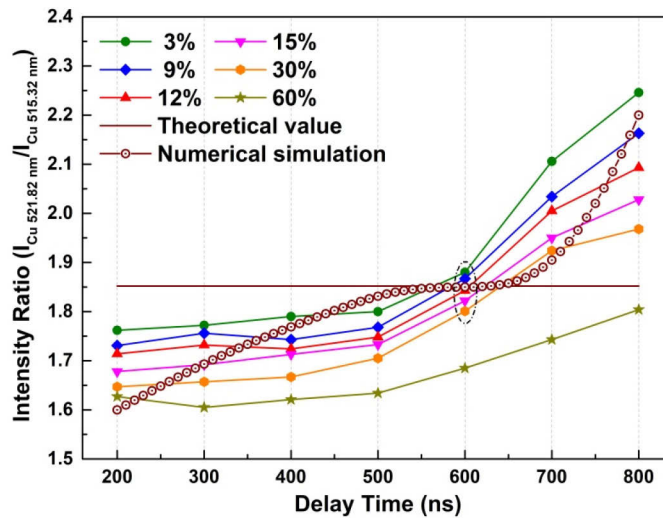
Fig. 1. Relationships between  $K$  and  $T$  corresponding to Cu I 521.82 nm and Al I 396.15 nm.

Figure 3 shows the temporal evolutions of  $I_{\text{Cu } 521.82 \text{ nm}}/I_{\text{Cu } 515.32 \text{ nm}}$  within 200–800 ns measured by using the copper-containing tablets. The straight line represents the theoretical ratio of 1.85, and the lifetime of this Cu I doublet is  $\sim 800$  ns. As can be seen, all the curves show an upward trend. The optimal delay time increase with the increase of Cu content, and within the content range of 3–30%, the Cu I doublet could be regarded as quasi-optically thin at the corresponding optimal delay time (circled by dotted ellipses). However, when the Cu content was larger than 60%, the quasi-optically thin doublet could never be captured during the lifetime of plasma. By non-linear fitting between optimal delay time and Cu content, the maximum Cu content corresponding to the selected line that could be considered as quasi-optically thin during the plasma lifetime was 50.7%. It means that when the Cu content is larger than 50.7%, the quasi-optically thin lines can never be captured for the selected line during the lifetime of plasma and the corresponding optimal times for samples with content larger than 50.7% can only be predicted through the non-linear fitting. The curve of wine hollow dot circles in Fig. 3 is a numerical simulation of temporal evolution of Cu I doublet intensity ratio using the first



**Fig. 2.** Relationships between  $y$  and  $x$  corresponding to the Cu I doublet and the Al I doublet, where  $x = K_1/\Delta\lambda_0$ , and  $y=(SA_1)'SA_2-(SA_2)'SA_1$ .

derivative data shown in Fig. 2 with an initial value of 1.6. As can be seen, the trend of this simulated curve is basically consistent with the experimental results.



**Fig. 3.** Temporal evolutions of  $I_{Cu\ 521.82\ nm}/I_{Cu\ 515.32\ nm}$  with Cu content in the range of 3–60%.

#### 4.2. Evolution of doublet Al I intensity ratio

Similar to the Cu I spectral line, the numerical fitting curve of  $K$  versus  $T$  corresponding to Al I 396.15 nm is shown as blue dash dot curve in Fig. 1. Here the  $K$  for Al increases with the decrease of  $T$ , that is,  $K$  increases with time, so  $K' > 0$ . Then the derivative of the intensity ratio  $I_{Al\ 396.15\ nm}/I_{Al\ 394.40\ nm}$  with respect to time can be determined by Eq. (9), and  $C_2=0.496$ . The relationship of  $y$  with respect to  $x$  for the Al I doublet was shown as blue dash dot curve in Fig. 2.

It can be seen that  $y$  is always negative, and tends to be zero when  $x$  is low to 0 (optically thin) or higher than 20 (serious self-absorption), which means that, in theory, the doublet ratio of Al I decreases with time and the trend tends to be zero in the case of optically thin or serious self-absorption. Therefore, the doublet Al I intensity ratio falls with time, and its trend tends to zero as the self-absorption decreases to optically thin. Then it begins to fall again with the increase of self-absorption until the change tends to zero when the self-absorption is serious.

Figure 4 shows the temporal evolution of  $I_{\text{Al } 396.15 \text{ nm}}/I_{\text{Al } 394.40 \text{ nm}}$  within 200–2000 ns measured by using the aluminum-containing tablets. The straight line represents the theoretical ratio of 1.97. The results indicate that all the curves show a downward trend and the optimal delay time decreases with the increase of Al content. The Al I doublet could be regarded as quasi-optically thin at the corresponding optimal delay time within the content range of 5–13%. However, when the Al content was larger than 19%, the quasi-optically thin doublet could never be captured during the acquisition period of plasma. The exponential fitting between optimal delay time and Al content showed that due to the poor signal-to-noise ratio of plasma spectra recorded before 200 ns, the maximum Al content corresponding to the selected line that could be considered as quasi-optically thin was 15.9%. It means that when the Al content is larger than 15.9%, the quasi-optically thin lines can never be captured for the selected line after 200 ns and the corresponding optimal times for samples with content larger than 15.9% can only be predicted through exponential fitting. The curve of wine hollow dot circles in Fig. 4 is a numerical simulation of temporal evolution of Al I doublet intensity ratio using the first derivative data shown in Fig. 2 with an initial value of 2.15. As can be seen, the trend of this simulated curve is basically consistent with the experimental results.

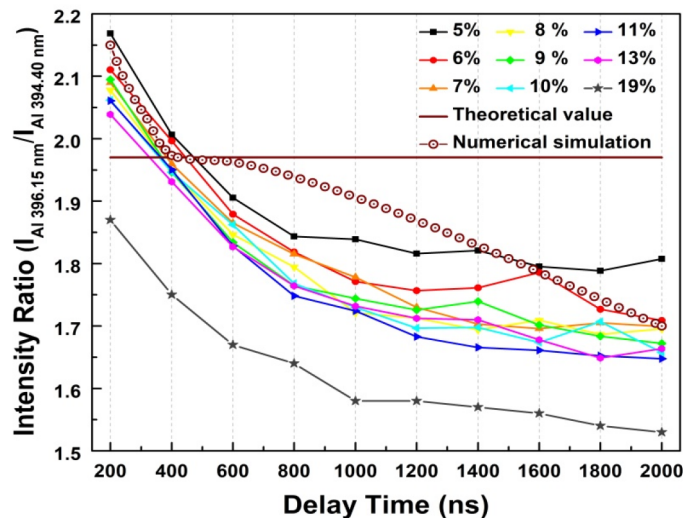


**Fig. 4.** Temporal evolutions of  $I_{\text{Al } 396.15 \text{ nm}}/I_{\text{Al } 394.40 \text{ nm}}$  with Al content in the range of 5–19%.

#### 4.3. Spectral line selection criterion

The above analysis shows that, under the assumptions that the plasma is uniform and in LTE, and the area density remains unchanged, the curve of doublet intensity ratio theoretically presents a monotonic trend. Thus, in order to verify the applicability of SAF-LIBS for quantitative analysis in a certain field, it is necessary to measure the doublet intensity ratios at both the initial and final stages of plasma that generated from the boundary sample with the highest element content. Only when the theoretical value is between the two measured ratios, the selected doublet can reach

quasi-optically thin during plasma evolution and is suitable for SAF-LIBS measurement. The above method can be used as a criterion for rapid spectral line selection in practical application of SAF-LIBS. For example, in our experiments, the intensity ratios of the Cu I 521.82 and 515.32 nm doublet for the 30% copper-containing tablet at 200 ns and 800 ns are on the both sides of the theoretical ratio 1.85, which indicates that this Cu I doublet can reach quasi-optically thin during the plasma evolution and is suitable for SAF-LIBS analysis of samples with 0–30% copper content. However, for the 60% copper-containing tablet, both the doublet intensity ratios are lower than the theoretical value, indicating that this Cu I doublet is not suitable for SAF-LIBS analysis of samples containing more than 60% copper.

## 5. Conclusion

SAF-LIBS can easily and directly obtain quasi-optically thin lines without any correction or auxiliary means. However, how to select the right doublet lines for a certain analytical element accurately and quickly is the bottleneck to be solved in the practical application of this technology. In this work, the self-absorption process in plasma and the trends of doublet intensity ratio for different electronic transitions are analyzed. The theoretical analysis and experimental verification of Cu I and Al I doublets show that the evolution trend of doublet intensity ratio is monotonous under the assumption that the plasma is uniform and in LTE, and the area density is a constant. A selection criterion of spectral line for SAF-LIBS applications is derived as follows: only when the doublet intensity ratios measured at the initial and final stages of plasma induced by the boundary sample with the highest element content lie on both sides of the theoretical ratio, the doublet lines can reach quasi-optically thin during plasma evolution and are suitable for SAF-LIBS measurements. This rapid spectral line selection criterion is expected to promote the practical application of SAF-LIBS technology.

## Funding

National Key R&D Program of China (2017YFA0304203); Changjiang Scholars and Innovative Research Team in University of Ministry of Education of China (IRT\_17R70); National Natural Science Foundation of China (11434007, 61475093, 61775125, 61875108, 61975103); Major Special Science and Technology Projects in Shanxi (201804D131036, MD2016-01); 111 project (D18001); Fund for Shanxi “1331KSC”.

## References

1. Z. Wang, T. B. Yuan, Z. Y. Hou, W. D. Zhou, J. D. Lu, H. B. Ding, and X. Y. Zeng, “Laser-induced breakdown spectroscopy in China,” *Front. Phys.* **9**(4), 419–438 (2014).
2. K. Aryal, H. Khatri, R. W. Collins, and S. Marsillac, “In situ and ex situ studies of molybdenum thin films deposited by RF and DC magnetron sputtering as a back contact for CIGS solar cells,” *Int. J. Photoenergy* **2012**(1), 1–7 (2012).
3. Z. Wang, L. Z. Li, L. West, Z. Li, and W. D. Ni, “A spectrum standardization approach for laser-induced breakdown spectroscopy measurements,” *Spectrochim. Acta, Part B* **68**(2), 58–64 (2012).
4. M. Gaft, E. Dvir, H. Modiano, and U. Schone, “Laser induced breakdown spectroscopy machine for online ash analyses in coal,” *Spectrochim. Acta, Part B* **63**(10), 1177–1182 (2008).
5. S. C. Yao, J. D. Lu, K. Chen, S. H. Pan, J. Y. Li, and M. R. Dong, “Study of laser-induced breakdown spectroscopy to discriminate pearlitic/ferritic from martensitic phases,” *Appl. Surf. Sci.* **257**(7), 3103–3110 (2011).
6. H. Amamou, A. Bois, B. Ferhat, R. Redon, B. Rossetto, and P. Matheron, “Correction of Self-Absorption Spectral Line and Ratios of Transition Probabilities for Homogenous and LTE Plasma,” *J. Quant. Spectrosc. Radiat. Transfer* **75**(6), 747–763 (2002).
7. R. Hai, N. Farid, D. Y. Zhao, L. Zhang, J. H. Liu, H. B. Ding, J. Wu, and G. N. Luo, “Laser-induced breakdown spectroscopic characterization of impurity deposition on the first wall of a magnetic confined fusion device: experimental advanced superconducting tokamak,” *Spectrochim. Acta, Part B* **87**(87), 147–152 (2013).
8. J. P. Singh and S. N. Thakur, *Laser-Induced Breakdown Spectroscopy* (Elsevier Press, Cambridge, 2007).
9. H. Amamou, A. Bois, B. Ferhat, R. Redon, B. Rossetto, and M. Ripert, “Correction of the Self-Absorption for Reversed Spectral Lines: Application to Two Resonance Lines of Neutral Aluminum,” *J. Quant. Spectrosc. Radiat. Transfer* **77**(4), 365–372 (2003).

10. F. Bredice, F. O. Borges, H. Sobral, M. Villagran-Muniz, H. O. Di Rocco, G. Cristoforetti, S. Legnaioli, V. Palleschi, L. Pardini, A. Salvetti, and E. Tognoni, "Evaluation of Self-Absorption of Manganese Emission Lines in Laser Induced Breakdown Spectroscopy Measurements," *Spectrochim. Acta, Part B* **61**(12), 1294–1303 (2006).
11. A. M. El Sherbini, Th. M. El Sherbini, H. Hegazy, G. Cristoforetti, S. Legnaioli, V. Palleschi, L. Pardini, A. Salvetti, and E. Tognoni, "Evaluation of self-absorption coefficients of aluminum emission lines in laser-induced breakdown spectroscopy measurements," *Spectrochim. Acta, Part B* **60**(12), 1573–1579 (2005).
12. L. Sun and H. Yu, "Correction of Self-Absorption Effect in Calibration-Free Laser Induced Breakdown Spectroscopy by Induced Reference Method," *Talanta* **79**(2), 388–395 (2009).
13. B. A. Alfarraj, C. R. Bhatt, F. Y. Yueh, and J. P. Singh, "Evaluation of Optical Depths and Self-Absorption of Strontium and Aluminum Emission Lines in Laser-Induced Breakdown Spectroscopy (LIBS)," *Appl. Spectrosc.* **71**(4), 640–650 (2017).
14. T. Q. Li, Z. Y. Hou, Y. T. Fu, J. L. Yu, W. L. Gu, and Z. Wang, "Correction of self-absorption effect in calibration-free laser-induced breakdown spectroscopy (CF-LIBS) with blackbody radiation reference," *Anal. Chim. Acta* **1058**(13), 39–47 (2019).
15. J. J. Hou, L. Zhang, W. B. Yin, S. C. Yao, Y. Zhao, W. G. Ma, L. Dong, L. T. Xiao, and S. T. Jia, "Development and performance evaluation of self-absorption-free laser-induced breakdown spectroscopy for directly capturing optically thin spectral line and realizing accurate chemical composition measurements," *Opt. Express* **25**(19), 23024–23034 (2017).
16. J. J. Hou, L. Zhang, Y. Zhao, W. G. Ma, L. Dong, W. B. Yin, L. T. Xiao, and S. T. Jia, "Resonance/non-resonance doublet-based self-absorption-free LIBS for quantitative analysis with a wide measurement range," *Opt. Express* **27**(3), 3409–3421 (2019).
17. D. Bulajic, M. Corsi, G. Cristoforetti, S. Legnaioli, V. Palleschi, A. Salvetti, and E. Tognoni, "A procedure for correcting self-absorption in calibration free-laser induced breakdown spectroscopy," *Spectrochim. Acta, Part B* **57**(2), 339–353 (2002).
18. Y. Tang, J. Li, Z. Hao, S. Tang, Z. Zhu, L. Guo, X. Li, X. Zeng, J. Duan, and Y. Lu, "Multielemental selfabsorption reduction in laser-induced breakdown spectroscopy by using microwave-assisted excitation," *Opt. Express* **26**(9), 12121–12130 (2018).